Pre-straining as an effective strategy to mitigate ratcheting during fatigue in flax FRP composites for structural applications

Valentin Perruchoud [1], René Alderliesten [2], Yasmine Mosleh [1]

[1] Biobased Structures and Materials, Faculty of Civil Engineering and Geosciences, Delft University of Technology, the Netherlands (v.p.perruchoud@tudelft.nl)

[2] Aerospace Structures and Materials, Faculty of Aerospace Engineering, Delft University of Technology, the Netherlands

Biobased fibre-reinforced polymer (FRP) composites, consisting of natural lignocellulosic fibres such as flax or hemp, are great alternatives to synthetic fibres to mitigate the environmental impact of high-performance composites in engineering structures. Natural fibres such as flax have damping and specific mechanical properties suitable to potentially replace glass fibres in FRP composites in engineering structures. However, structural design with flax FRPs can be challenging for engineers due to their rather peculiar mechanical responses thanks to the complex multi-scale microstructure of the flax fibres. In particular, flax FRP composites have shown large ratcheting (accumulation of plastic deformation) and stiffness increase when subjected to tensile fatigue loading. Therefore, this paper proposes a novel yet simple 'pre-straining' method as a promising strategy for improving the fatigue response of flax FRP, to potentially replace synthetic glass FRP in various engineering structures. To this end, cross-ply flax, and glass FRP composite laminates were manufactured and subsequently tensile-tensile fatigue experiments were performed. It was observed that pre-straining of flax FRP composite coupons can improve their mechanical performance by increasing stiffness and reducing ratcheting during fatigue which is attributed to further alignment of the fibres within the twisted yarns, as well as possible microfibril alignment. The pre-straining of glass fibre reinforced composites samples did not lead to any remarkable reduction in ratcheting nor increase in stiffness.

Keywords: Bio-composite, fatigue, pre-straining, ratcheting, tensile loading, damage

1 Introduction

In the relentless pursuit of performance in the field of structural engineering, fibre-reinforced polymer composites (FRPs) have emerged as the most compelling option for stiff, strong, and lightweight structural design. With all the mentioned qualities, the use of FRPs extends to a broad spectrum of application areas such as aerospace, marine, wind energy, and construction. Currently, the most widely used fibres in structural FRPs are synthetic fibres such as glass and carbon fibres. In particular, glass fibres are the ones preferred in the construction industry, an application area which generally requires large amount of material for structures such as bridges and wind turbine blades [1], [2], [3]. Carbon fibres are generally preferred for aeronautical applications such as plane wings where the additional cost of carbon fibres is justified by the weight savings thanks to the very high specific strength and stiffness of carbon fibres [4].

Despite all the above-mentioned qualities, the synthetic FRPs adopted by multiple industries have their shortcomings, particularly when it comes to sustainability. Indeed, manufacturing of both glass and carbon fibres requires intricate processes that demand high energy and the use of non-renewable resources. Furthermore, at the end of life of a synthetic FRP structure, disposal or incineration of the materials is environmentally damaging and the recycling pathways are rather complex. For these reasons, many researchers and industries have expressed interest in biobased FRPs that can provide a sustainable, environmentally friendly alternative to synthetic FRPs and other traditional construction materials while offering competitive specific mechanical properties [5].

Research investigating flax FRP composites (FFRPs) as an alternative to glass FRP composites (GFRPs) in applications subjected to fatigue loading has already been conducted. Case studies involving wind turbine blades [6], [7] and railway axle ties [8] have illustrated the viability of FFRP as a practical choice for structural applications. Studies on the fatigue life of FFRP and GFRP coupons [9], [10] indicate that FFRP exhibits a more stable fatigue performance, evidenced by a smaller slope on the S-N curve compared to GFRP. However, those fatigue studies have also highlighted a drawback of FFRP for fatigue applications with a strong ratcheting effect [11] (accumulation of plastic deformations) in laminates containing 0° plies which is not seen in GFRP. This ratcheting effect is undesirable for structural design as long-term deformations have to be taken into account in addition to creep. Remarkably for FFRP, this ratcheting effect is coupled with a stiffening effect as the modulus of the coupons increases during fatigue which contradicts the observations in GFRP where the modulus is consistently decreasing with the accumulation of damage in fatigue [12].

The strong ratcheting and the stiffness increase observed in FFRP composites during cyclic loading could be attributed to the complex hierarchical microstructure of flax fibres, and manufactured flax yarns. Each technical flax fibre is a bundle of elementary fibres held together by a pectin rich middle lamella layer. Each elementary fibre comprises of a hollow central channel (lumen) surrounded by primary and secondary cell walls. The cell walls are composites of crystalline cellulose micro/nano fibrils embedded in a matrix of lignin and hemicellulose [13]. The cellulose microfibrils form some angle with the main axis of the elementary flax fibre, and may therefore be reoriented with the application of a tensile load [14]. Additionally, on a higher yarn scale, the application of a tensile load may also induce reorientation as flax yarns have a twist angle introduced by spinning, an integral part of their manufacturing.

This paper introduces a straightforward and yet effective method to enhance the tensile fatigue performance of FFRPs through the implementation of pre-straining. The rationale behind pre-straining is derived from the following insights: First, the accumulation of progressive deformation or ratcheting observed in FFRPs under fatigue loading is an undesirable mechanical response for structural engineering. Next, ratcheting in FFRPs may be attributed to microfibrils reorientation, or yarn untwisting, or a combination of both. Further, this reorientation of microfibrils and/or yarns inside FFRPs may also be achieved through quasi-static tensile loading. Consequently, we propose the following hypothesis for FFRPs with fibres parallel to the direction of an applied tensile load: *Applying a strain exceeding that experienced during fatigue before subjecting the material to fatigue loading enhances its fatigue mechanical performance by reducing ratcheting and stiffness variation throughout its fatigue life.*

To validate the aforementioned hypothesis, an experimental campaign was conducted to compare the fatigue response of a pristine and a pre-strained FFRP laminate. The fatigue response was measured by strain, modulus, work, as well as microstructure damage using destructive optical microscopy. For the purpose of understanding the effect of pre-straining with different types of fibre reinforcement, the experimental campaign also involved testing pristine and pre-strained GFRP laminates with the same matrix as in the FFRP laminates.

2 Materials and methods

2.1 Composites Specimens

2.1.1 Composite laminate architecture

The FFRP specimens used in this research are coupons 2.8 mm thick cut in a dogbone shape according to Figure 1 to prevent failure at the edge of the clamps during fatigue. The strain measurements are taken by an extensometer in the narrow cross-section. The FFRP laminate consists of 6 layers of Bcomp quasi-unidirectional flax mat Amplitex 280 g/m^2 arranged in the symmetrical lay-up $[0/90/0]_S$. The selection of this lay-up configuration was motivated by the interest to investigate the mechanical response of flax fibres when subjected to loading along their primary axis, leading to the inclusion of 0° layers. While the use of a strictly unidirectional lay-up was considered, preliminary testing revealed susceptibility to fatigue-induced splitting in such specimens. Consequently, 90° layers were incorporated to mitigate the occurrence of splitting phenomena.

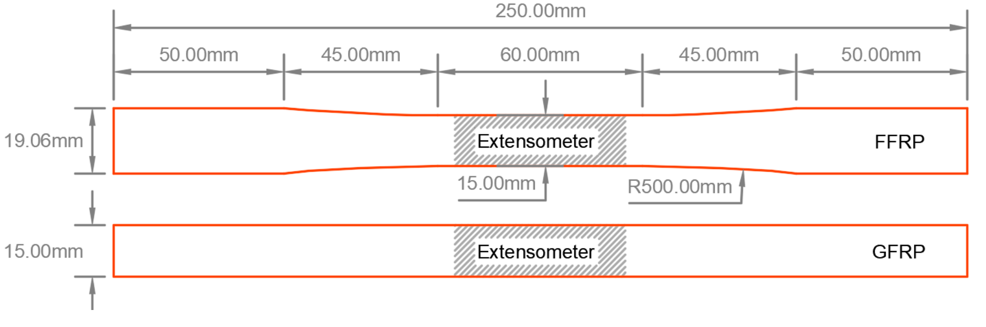

Figure 1. Geometry of FFRP and GFRP specimens

For GFRP, a rectangular geometry was chosen as GFRP specimens did not reach premature failure at the tabs during fatigue experiments, thus clamp failure was not an issue. The GFRP laminate consists of 3 layers of quasi-UD Kush Synthetics High stiffness glass fabric 1260 g/m^2 arranged in the lay-up [0/90/0] resulting in a laminate thickness of 2.9 mm. A laminate of 3 layers was chosen to keep the same ratio of fibres in the 0° and 90° direction as in FFRP and obtain a similar total laminate thickness.

For the sake of isolating the effect of fibres in the comparison of FFRP and GFRP, the same Swancor 2511-1AL/BL epoxy resin system is used as matrix for both composites.

2.1.2 Manufacturing

GFRP and FFRP plates were manufactured using a vacuum assisted resin infusion process followed by an 18 hours, 70°C, 7 bars autoclave post-cure. The plates were then cut into the test coupons with the use of a waterjet cutter. Differential scanning calorimetry (DSC) was used at the end of the manufacturing process to verify the completion of the resin cure by performing three heating/cooling cycles between 0°C and 150°C and measuring the endothermal peaks to ensure that the glass transition temperature (Tg) was not shifting by more than 3°C. Optical microscopy was used to ensure cracks or voids significant in comparison to fatigue damage were not present in the microstructure of pristine specimens (qualitative assessment). The fibre volume fraction was estimated at 42% and 53% for FFRP and GFRP respectively based on calculations with the density of the fibre mats, epoxy resin, and composites.

*2.2 **Mechanical testing***

2.2.1 Pre-straining procedure

Pre-straining was applied with 2 mm/min displacement-controlled loading in a tensile testing machine. For FFRP, pre-straining was applied up to a strain of 1.6%. At this strain level, the tensile stress corresponds to 80% of the FFRP quasi-static ultimate tensile strength (UTS). Subsequently, a displacement of -2 mm/min was applied until the tension was released as shown in Figure 2. Reaching 80% of the FFRP UTS ensured that the maximum strain reached during pre-straining was larger than the maximum strain reached during fatigue.

To load GFRP to the same specific stress as FFRP, the same pre-straining procedure was applied but the maximum load applied on GFRP was defined as the load applied on FFRP multiplied by a factor of 1.6 to account for the difference in density. This corresponded to a maximum GFRP strain in pre-straining of 0.9%. This correlation with density is used to compare the pre-straining and fatigue response of the composites by assuming they are employed in a similar application, where the stresses are proportional to the weight of the structure.

2.2.2 *Fatigue testing procedure*

Tension-tension fatigue tests were conducted under force control mode with a loading ratio of R = 0.1 and a frequency of 5 Hz. For FFRP, the maximum load was 60% of UTS. To load GFRP to the same specific stress as FFRP, the maximum and minimum load applied to FFRP were multiplied by a factor of 1.6 and applied to GFRP corresponding to 32% of the GFRP UTS. Each fatigue test was replicated 6 times, 3 times on pristine samples and 3 times on pre-strained samples.

2.2.3 *Test setup for pre-straining and fatigue*

Pre-straining and fatigue tests were performed on an Instron 1251 100 kN fatigue tensile testing machine equipped with hydraulic clamps. A climate chamber encloses the testing area ensuring that the testing environment remains at a constant 20°C and 50% RH. The force was captured by the load cell of the tensile testing machine. The specimen strain was captured by an extensometer attached on the narrow cross-section of the specimen. During fatigue testing, 50 data points of force and strain were recorded for each of the 500 first loading cycles and then once every 1’000 cycles.

2.3 ***Analysis of fatigue experimental data***

2.3.1 *Calculation of dynamic modulus and ratcheting*

The dynamic modulus E^{D} and ratcheting ε^{r} are calculated for each recorded cycle according to definition shown in Figure 2. As the deformation on the first fatigue loading cycle can vary specimen-to-specimen, the second fatigue loading cycle is taken as reference for both E^{D} and ε^{r} . Plots in the results section for the dynamic modulus are expressed as the ratio $E_i^{\mathrm{D}}/E_2^{\mathrm{D}}$ to describe the variation of stiffness throughout fatigue life. Similarly for ratcheting, the plots of ε^{r} express the evolution of ratcheting during fatigue life.

2.3.2 *Calculation of strain energy release*

The total work w_i^{T} , area under the loading curve, and the inelastic work w_i^{P} , area inside of the hysteresis, are computed for each recorded cycle, as described in Figure 3. In the results section, the work plots are expressed with the ratio $w_i^{\mathrm{P}}/w_i^{\mathrm{T}}$ describing how much strain energy is released (dissipated) at each cycle relative to the total work performed on the material during the load increasing part of the cycle. This ratio serves as a damage indicator, offering insights into the extent of damage or reorganisation occurring within specimens. This metric may complement optical microscopy observations, which are limited to detecting specific types of cracks and require the destruction of the specimens.

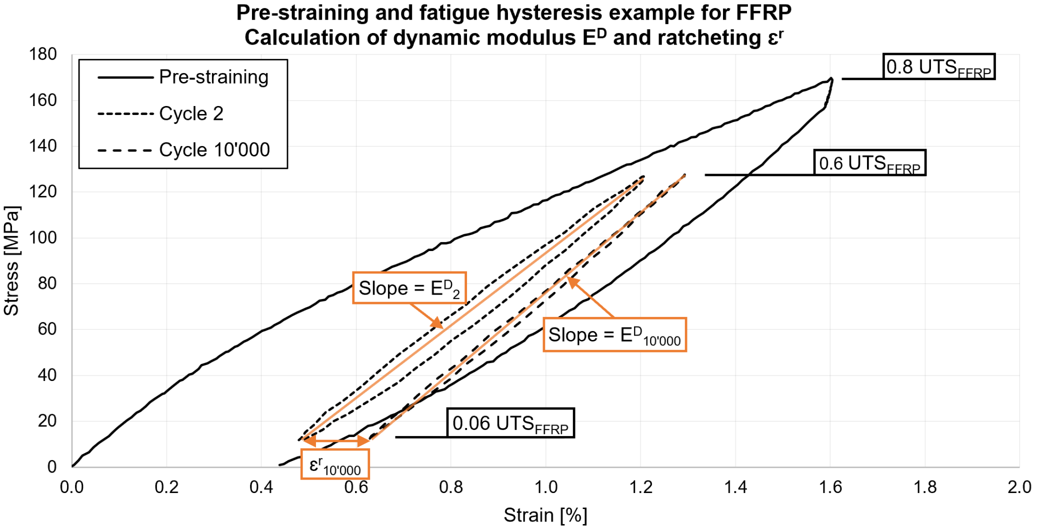

Figure 2. Definition of dynamic modulus and permanent strain with example of pre-straining and fatigue hysteresis

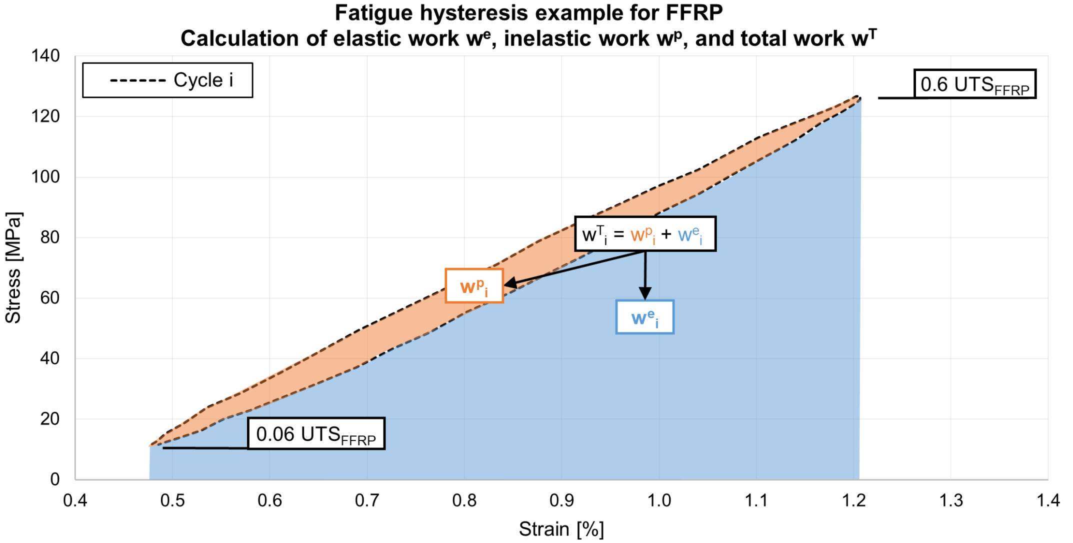

Figure 3. Definition of elastic, inelastic and total work calculation for each cycle i

2.4 *Optical microscopy*

Microscopy samples were cut from pristine and mechanically tested GFRP and FFRP specimens in their narrow cross-section. In the case of specimens reaching failure, the microscopy samples were taken at least 5 mm away from the final fracture. Then, the samples were embedded in a resin on the cut side or rotated by 90° to observe cracking in the 0° plies and 90° plies respectively. Grinding and polishing was performed automatically with a Struers Tegramin-20 using the *Epoxy soft and ductile* program for FFRP and *Fibers – fragile fibres* program for GFRP. A Keyence laser confocal VK-X3000 was used to capture optical images at different magnifications.

3 Results and discussion

3.1 *Mechanical response with and without pre-straining*

3.1.1 Pre-straining effect on dynamic modulus

The dynamic modulus was computed on pristine and pre-strained FFRP and GFRP specimens during fatigue testing. The GFRP tests showed no failure after 1’000’000 cycles at which point, they were stopped manually due to time constrains. All the FFRP specimens reached failure between 47’000 and 136’000 cycles. The evolution of the dynamic modulus is plotted in Figure 4 and its absolute values obtained at the cycle 2 and 10’000 are shown in Table 1.

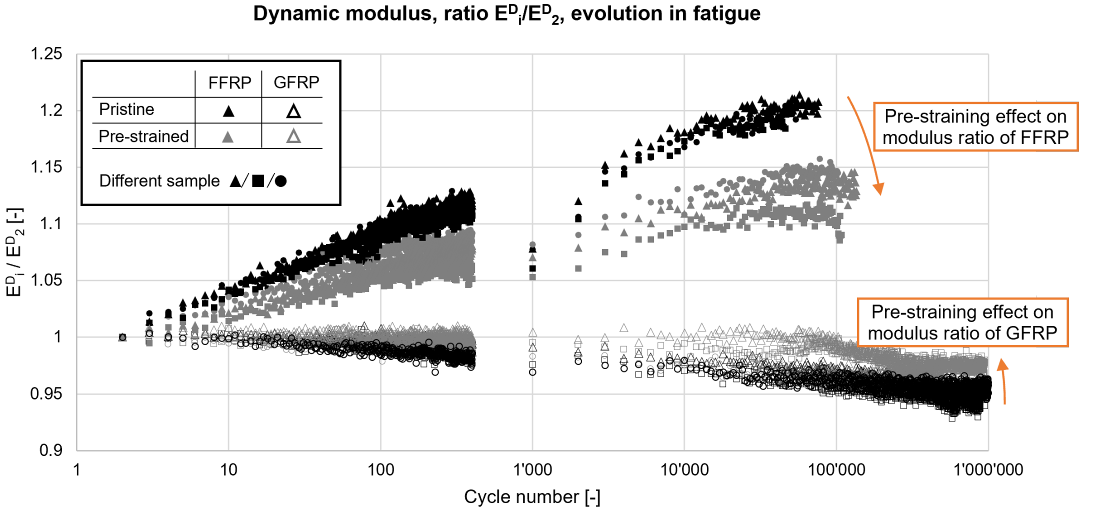

Figure 4. Evolution of dynamic modulus ratio throughout fatigue of FFRP and GFRP with and without pre-straining effect

Table 1. Values of dynamic modulus at 2 and 10'000 fatigue cycles for each test

	FFRP						GFRP					
	Pristine			Pre-strained			Pristine			Pre-strained		
Sample	1	2	3	1	2	3	1	2	3	1	2	3
E^{D}_{2} [GPa]	14.1	13.6	14.0	14.7	15.7	15.0	32.7	33.4	32.9	32.7	32.0	31.7
$E^{D}_{10'000}$ [GPa]	16.5	16.1	16.4	16.2	17.3	16.6	32.0	32.4	32.3	32.9	31.9	30.9
$E^{D}_{10'000} - E^{D}_{2}$ [GPa]	2.4	2.5	2.4	1.5	1.6	1.6	-0.7	-1.0	-0.6	0.2	-0.1	-0.8

In Figure 4, we observe an evolution of the dynamic modulus during fatigue in agreement with literature [12, 15] manifested by an increase for FFRP and decrease for GFRP. As hypothesized in the introduction, pre-straining significantly reduces the dynamic modulus variation of FFRP. Additionally, while the absolute values of dynamic modulus for pre-strained are higher than pristine (as result of pre-straining), the pristine samples exhibit a higher increase in modulus (i.e. $E_i^{\mathrm{D}} / E_2^{\mathrm{D}}$). For GFRP, Figure 4 suggests that pre-straining also reduces the variation of dynamic modulus during the fatigue life. In contrast to FFRP, this is achieved by minimizing the decline in the dynamic modulus. The absolute values of the dynamic modulus of FFRP and GFRP for cycle 2 and 10’000 are shown in Table 1.

3.1.2 *Pre-straining effect on ratcheting*

The ratcheting was computed for pristine and pre-strained FFRP and GFRP specimens during fatigue testing. The evolution of ratcheting is plotted in Figure 5 and the absolute values of plastic strains obtained at cycle 2 and 10’000 are shown in Table 2.

For both FFRP and GFRP, pre-straining seems to reduce the ratcheting by a factor of approximately 2 throughout the fatigue life (Fig. 5). However, it must be considered that the pre-straining effect expressed in absolute strain value is about an order of magnitude larger in FFRP than in GFRP. For the latter, the deformation due to ratcheting is small relative to elastic deformation. The values of ratcheting for FFRP and GFRP after 10’000 cycles ($\varepsilon^{r}_{10'000}$) are shown in Table 2.

Table 2. Values of plastic strain at 2 and 10'000 cycles for each fatigue test

	FFRP						GFRP					
	Pristine			Pre-strained			Pristine			Pre-strained		
Sample	1	2	3	1	2	3	1	2	3	1	2	3
ε_{2} [%]	0.20	0.22	0.19	0.57	0.49	0.55	0.07	0.07	0.07	0.38	0.09	0.08
$\varepsilon_{10'000}$ [%]	0.56	0.60	0.56	0.74	0.63	0.73	0.09	0.10	0.09	0.39	0.09	0.10
$\varepsilon^{r}_{10'000}$ [%]	0.36	0.38	0.37	0.17	0.14	0.18	0.02	0.03	0.03	0.01	0.00	0.02

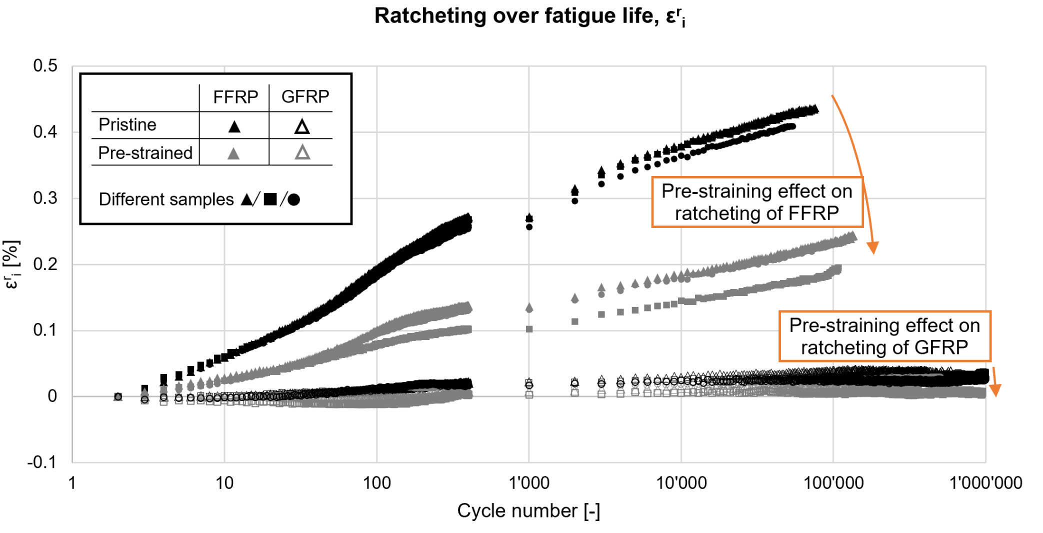

Figure 5. Evolution of ratcheting throughout fatigue of FFRP and GFRP with and without pre-straining effect

3.1.3 *Pre-straining effect on fatigue life of FFRP*

The comparison of the number of loading cycles to failure in pristine and pre-strained FFRP specimens shows that pre-straining increase fatigue life (Table 3). This increase in fatigue life could be related to the increased stiffness reducing the amount of strain energy applied in each loading cycle, thus reducing the damage accumulating with each fatigue cycle.

Table 3. Number of loading cycles to failure for FFRP specimens

	FFRP	
Sample	**Pristine**	**Pre-strained**
1	*54'962*	*102'160*
2	*82'159*	*108'972*
3	*47'170*	*136'103*

3.1.4 *Analysis of FFRP fatigue response*

With the elongation of FFRP specimens, whether due to the pre-straining or repeated fatigue loading cycles, an increase in dynamic modulus is observed which contradicts the basic assumptions of stiffness degradation made in numerous fatigue life models for FRP composites [16], [17], [18], [19], [20]. Behind the stiffness degradation assumption based on continuum damage mechanics (CDM) used in these models is the nucleation and growth of microcracks (within the matrix and at the fibre/matrix interface) developing during fatigue, thus degrading the stiffness of the composite. This stiffness degradation has been experimentally verified in literature for synthetic FRP composites [21], [22] and it is further confirmed given the GFRP results in the present study (Fig. 4) and the microscopy observations showing microcracks due to fatigue loading in Figure 6. Paradoxically, microcracks due to fatigue are also observed in FFRP composites (Fig. 7) and yet their stiffness is consistently increasing during fatigue.

With microcracks appearing and stiffness increasing, an explanation for the FFRP mechanical response must rely on a phenomenon increasing the apparent modulus of the composite despite a reduction of internal fibre/matrix interfacial surface for stress transfer. While the explanation of the phenomenon is not known yet, two hypothesis based on an alignment of the flax fibres can be formulated.

The first hypothesis, at the composite microstructure scale, relies on the alignment of the flax yarns in the 0° plies. An alignment of the technical fibres in the flax yarns can happen in the specimens tested because contrary to the single glass fibres in the glass fibre mat, technical flax fibres are twisted to form yarns for the manufacturing of flax fibre mats, misaligning the fibre axis and the loading axis. The fibre twist in FFRP and absence of fibre twist in GFRP are visible in Figure 7 and Figure 6 respectively. With cyclic tensile loading of the composite, the yarn twist angle may be reduced. Thus, reducing the angle between the loading direction and the flax fibre yarn axis could increase the effective modulus of the composite.

The second hypothesis, at the elementary flax fibre microstructure scale, relies on the alignment of the cellulose microfibrils being the main constituent of the elementary flax fibre cell walls. By nature, those microfibrils have an angle relative to the axis of the elementary flax fibre [23], [24]. Tensile testing on single elementary flax fibres have shown that the longitudinal Young's modulus of flax fibres increases with tensile deformation along the fibre, and it has been hypothesised that this is due to a further alignment of the microfibrils with respect to the loading direction. Consequently, the increase of the flax fibres modulus can be explained with a model considering the alignment of microfibrils [14]. Therefore, stiffening at the composite scale may also be explained by an alignment occurring in the microstructure of the elementary flax fibres.

3.2 *GFRP and FFRP microstructure damage patterns*

3.2.1 Fatigue induced damage

The comparison of images taken on pristine specimens and on specimens subjected to fatigue showed no easily identifiable fatigue cracks in the 0° plies. However, in the 90° plies, cracks perpendicular to the loading direction are systematically visible both in the GFRP and FFRP specimens. In the GFRP specimens, the cracks seem to nucleate in the fibre rich regions, propagate along the surface of individual glass fibres within the yarn and extend into the matrix rich regions. Similarly, in FFRP specimens, cracks nucleate in the yarns which are the fibre rich regions and propagate along the surface of elementary flax fibres, rarely extending to the matrix rich regions.

About the damage pattern in the 90° plies for both materials, cracks do not appear uniformly as small cracks following the surface of all fibres. Instead, a limited number of significant cracks are concentrated in specific locations, exhibiting a recurring pattern with cracks orientated perpendicular to the loading direction. In GFRP these cracks are spaced at a certain interval (Fig. 6). In the case of FFRP, a single crack is generally present in each yarn splitting the yarn (Fig. 7).

The damage patterns in the 90° plies are a consequence of the anisotropic nature of FRP composites, and the mismatch in fibre/matrix stiffness. As result of the inhomogeneity of FRP composites stress concentrations appear within the microstructure under load, triggering cracks releasing the stress concentration in specific locations. In the 90° plies, due to the much higher stiffness of particularly the glass fibres compared to the polymer matrix, strain magnification occurs between the fibres, leading to matrix cracks. Because of the small stiffness mismatch for flax fibres (their transverse modulus is similar to the matrix modulus) no matrix cracks should be expected. But due to the weak interlayer between the elementary fibres (the middle lamella), cracks may be expected inside the technical fibres (bundles of elementary fibres). This is especially visible within the yarns of the FFRP specimens. Additionally, it is hypothesised that the manufacturing process of FFRP may result in dry areas in-between fibres where no tensile load could be transferred fibre-to-fibre in the direction transverse to those fibres. Finally, the intrinsic chemical disparity between flax fibres and the matrix could also explain cracks in the fibre-rich regions of FFRP, as the interface strength between the fibre and matrix may be insufficient to support loading transverse to the fibres.

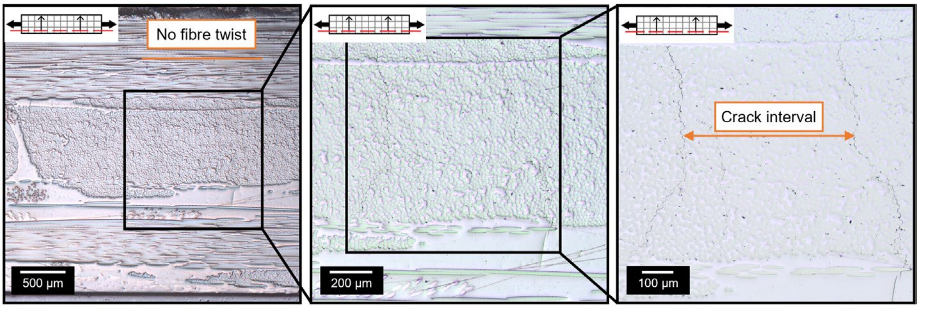

Figure 6. Optical microscopy of an GFRP specimen after fatigue in the 90° plies direction

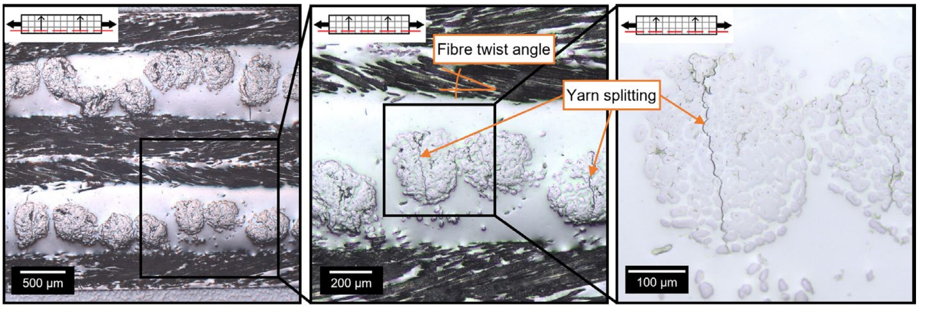

Figure 7. Optical microscopy of an FFRP specimen after fatigue in the 90° plies direction

3.2.2 *Pre-straining induced damage*

Some of the composite specimens were subjected to pre-straining and subsequently their microstructures were inspected by optical microscopy. Similar to fatigue loading induced damage patterns, pre-straining did not induce observable cracks in the 0° plies for either material but in the 90° plies, cracks of the same nature as those induced by fatigue can be detected. In GFRP, the pre-straining cracks look alike the cracks detected after fatigue with propagation from the fibre rich region to the matrix rich region (Fig. 8). In FFRP, the pre-straining cracks are less developed than the fatigue cracks (Fig. 9) with cracks only rarely crossing the full yarn which was systematically the case for fatigue cracks.

3.2.3 *Could pre-straining amplify fatigue induced damage?*

As pre-straining has been demonstrated to induce similar damage patterns as to fatigue loading in the composite microstructure, concerns may arise regarding the potential acceleration of damage growth in fatigue due to pre-straining. However, comparing damage features after fatigue in samples with and without pre-straining showed no

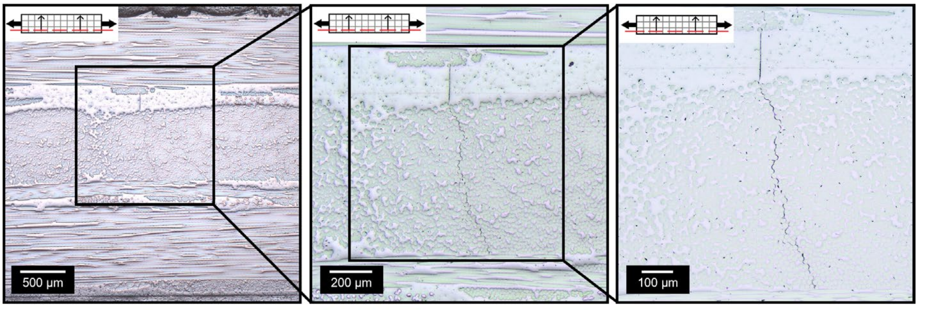

Figure 8. Optical microscopy of an GFRP specimen after pre-straining, view in the 90° plies direction

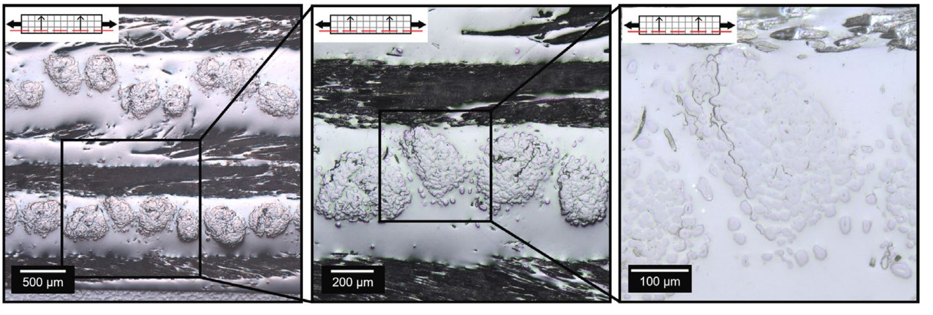

Figure 9. Optical microscopy of an FFRP specimen after pre-straining, view in the 90° plies direction

significant difference. In FFRP samples, cracks are typically confined to the yarns after fatigue testing with or without pre-straining. In GFRP samples, cracks tend to propagate from the fibre-rich region to the matrix-rich region after fatigue testing with or without pre-straining. It is important to note that the damage observed with optical microscopy only accounts for the 90° plies which do bear only a small portion of the total load compared to the 0° plies where no cracks have been detected.

3.3 *Global damage analysis with strain energy release*

The ratio of inelastic work w_i^{P} over total work w_i^{T}, both defined in Figure 3, expresses how much strain energy is dissipated through irreversible deformation, cracking, or friction relative to the amount of work applied. The development of this ratio of the entire fatigue life is illustrated in Figure 10. A smaller ratio is preferred for structural application as a ratio of 0 would yield a perfectly linear elastic material undamaged by loading cycles.

For GFRP, comparing the ratios of pristine and pre-strained specimens, this showed no benefits nor detrimental effects of pre-straining. On the other hand, pre-strained FFRP specimens showed a reduction of the ratio throughout the fatigue life, in particular towards the beginning of the fatigue life. Such a reduction of dissipated energy indicates that pre-straining has a beneficial effect for fatigue, because less damage is created at each loading cycle compared to the pre-strained specimen. As an advantage over microscopy observations, this metric also considers cracks too small to be detected by optical microscopy, whether they are in the 0° or 90° plies.

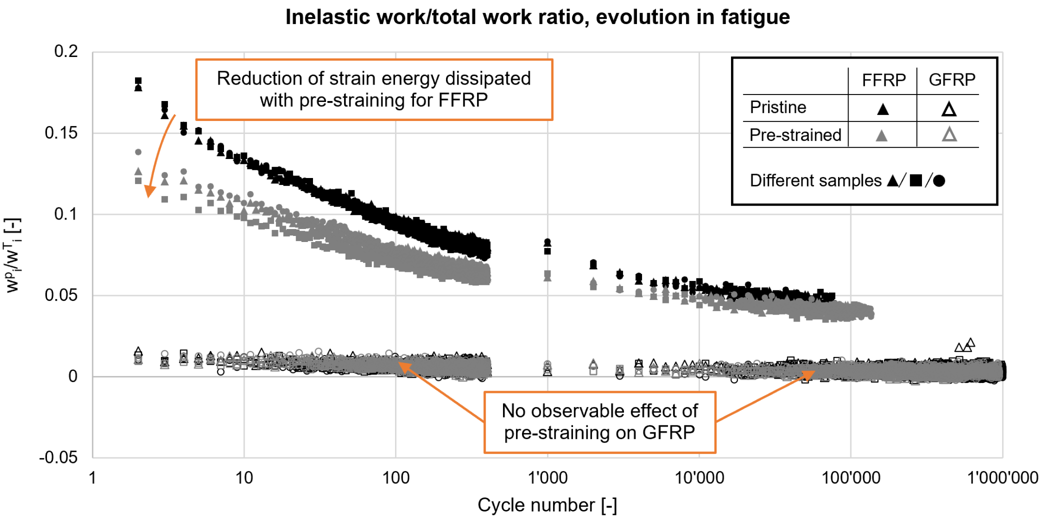

Figure 10. Strain energy dissipated in fatigue of FFRP and GFRP expressed as the ratio of inelastic work over total work for each loading cycle

3.4 ***Extension of pre-straining effects to creep performance of bio-composites***

In the context of the present experimental investigation, the efficacy of pre-straining is evaluated based on the tensile fatigue response only. Nevertheless, pre-straining or other equivalent pre-loading could also be employed to improve the FFRP response to other types of long-term mechanical loads such as creep which can be a concern for FFRP structures [25]. Indeed, due to creep concerns for a FFRP bridge in Ritsumasyl, Netherlands, the bridge deck was subjected to a pre-creep phase prior to entering service [26]. Though applied in different contexts, both pre-straining and pre-creep fundamentally revolve around the common concept of introducing permanent deformation into a structure before it enters into service. Consequently, both the short and long-term mechanical response of a FFRP structure could benefit from pre-straining or a similar process. The similarity of phenomena in FFRP composites is sometimes expressed in literature by describing ratcheting as creep-like behaviour [27].

4 Conclusion

In this investigation, we explored the efficacy of pre-straining as an effective strategy for biobased FRP composites to enhance their fatigue response in structural applications. For this we focused this investigation on cross-ply flax FRP composite laminates and studied cross-ply glass FRP composite laminates as a synthetic FRP benchmark. The study comprised an analysis of tensile fatigue responses of pristine and pre-strained FFRP and GFRP composite laminates along with microstructural damage analysis by optical inspection.

The findings reveal that pre-straining is a highly effective method for enhancing the fatigue response of flax FRP composites by reducing their ratcheting and simultaneously increasing their dynamic modulus and fatigue life. Importantly, this improvement is achieved without causing any more noticeable damage than the ones that occur during fatigue without pre-straining. By contrast, pre-straining created negligible effects on ratcheting and stiffness in the case of the GFRP composites.

With the pre-straining method proposed in this investigation, the undesirable effect of ratcheting for structural design can be mitigated prior to the structure entering service. It is crucial to note that pre-straining is advised only when a substantial portion of the flax fibres in the composite is loaded along or close to the main axis of the fibres as loading perpendicular to the fibres creates damage without substantial benefits to the fatigue response.

This study was limited to testing a single pre-straining and fatigue load level that allowed for the demonstration of pre-straining effects but is insufficient to select the appropriate pre-straining load for structural design. Additional testing with different levels of pre-straining and fatigue loading is necessary for the structural designer to make informed decisions on the level of pre-straining to apply and accurately predict the effect of pre-straining on fatigue life.

Given the observed benefits of pre-straining on the fatigue behaviour of flax FRP composites, it is recommended to incorporate this method in structural design to significantly improve the material's mechanical response to long-term service and improve competitiveness with synthetic counterparts like GFRP composites. This recommendation is not applicable to glass FRP composites as no noticeable benefits were observed with the application of pre-straining.

Acknowledgments

The authors wish to thank Laurens Bannier for his assistance in preparing specimens for mechanical testing as well as performing polishing and optical microscopy for the images presented in this paper. We also wish to thank Dr. Jaykarna Bhangale for offering and organizing the delivery of the epoxy resin used in the manufacturing of the specimens. Authors wish to sincerely thank the continuous support of all the technicians within the Macrolab/Stevinlaboratory of the faculty of Civil Engineering and Geosciences, and the ASM laboratory of the faculty of Aerospace Engineering at TU Delft.

Literature

[1] P. G. Kossakowski and W. Wciślik, "Fiber-Reinforced Polymer Composites in the Construction of Bridges: Opportunities, Problems and Challenges," *Fibers*, Vol. 10, No. 4, Art. No. 4, Apr. 2022, doi: 10.3390/fib10040037.

[2] J. Qureshi, "A Review of Fibre Reinforced Polymer Bridges," *Fibers*, Vol. 11, No. 5, Art. No. 5, May 2023, doi: 10.3390/fib11050040.

[3] L. Mishnaevsky, K. Branner, H. N. Petersen, J. Beauson, M. McGugan, and B. F. Sørensen, "Materials for Wind Turbine Blades: An Overview," *Materials* (Basel), Vol. 10, No. 11, p. 1285, Nov. 2017, doi: 10.3390/ma10111285.

[4] B. Parveez, M. I. Kittur, I. A. Badruddin, S. Kamangar, M. Hussien, and M. A. Umarfarooq, "Scientific Advancements in Composite Materials for Aircraft Applications: A Review," *Polymers*, Vol. 14, No. 22, Art. No. 22, Jan. 2022, doi: 10.3390/polym14225007.

[5] L. Yan, N. Chouw, and K. Jayaraman, "Flax fibre and its composites – A review," *Composites Part B: Engineering*, Vol. 56, pp. 296–317, Jan. 2014, doi: 10.1016/j.compositesb.2013.08.014.

[6] D. U. Shah, P. J. Schubel, and M. J. Clifford, "Can flax replace E-glass in structural composites? A small wind turbine blade case study," *Composites Part B: Engineering*, Vol. 52, pp. 172–181, Sep. 2013, doi: 10.1016/j.compositesb.2013.04.027.

[7] J. H. Lee, C. Collier, J. Ainsworth, K. N. Cho, and Y. S. Lee, "Development of Natural Fiber Wind Turbine Blades using Design Optimization Technology." *TEAM 2020*/21, Dec. 03, 2021.

[8] N. Graupner et al., "A Competitive Study of the Static and Fatigue Performance of Flax, Glass, and Flax/Glass Hybrid Composites on the Structural Example of a Light Railway Axle Tie," *Frontiers in Materials*, Vol. 9, 2022, Accessed: Mar. 22, 2023. [Online]. Available: https://www.frontiersin.org/articles/10.3389/fmats.2022.837289

[9] S. Liang, P.-B. Gning, and L. Guillaumat, "A comparative study of fatigue behaviour of flax/epoxy and glass/epoxy composites," *Composites Science and Technology*, Vol. 72, pp. 535–543, Mar. 2012, doi: 10.1016/j.compscitech.2012.01.011.

[10] F. Bensadoun, K. A. M. Vallons, L. B. Lessard, I. Verpoest, and A. W. Van Vuure, "Fatigue behaviour assessment of flax–epoxy composites," *Composites Part A: Applied Science and Manufacturing*, Vol. 82, pp. 253–266, Mar. 2016, doi: 10.1016/j.compositesa.2015.11.003.

[11] S. K. Paul, “A critical review of experimental aspects in ratcheting fatigue: microstructure to specimen to component,” *Journal of Materials Research and Technology*, Vol. 8, No. 5, pp. 4894–4914, Sep. 2019, doi: 10.1016/j.jmrt.2019.06.014.

[12] S. Liang, P.-B. Gning, and L. Guillaumat, “Properties evolution of flax/epoxy composites under fatigue loading,” *International Journal of Fatigue*, Vol. 63, pp. 36–45, Jun. 2014, doi: 10.1016/j.ijfatigue.2014.01.003.

[13] Z. Zhang et al., “High performances of plant fiber reinforced Composites—A new insight from hierarchical microstructures,” *Composites Science and Technology*, Vol. 194, p. 108151, Apr. 2020, doi: 10.1016/j.compscitech.2020.108151.

[14] C. Baley, “Analysis of the flax fibres tensile behaviour and analysis of the tensile stiffness increase,” *Composites Part A-applied Science and Manufacturing* - COMPOS PART A-APPL SCI MANUF, Vol. 33, pp. 939–948, Jul. 2002, doi: 10.1016/S1359-835X(02)00040-4.

[15] K. K. Singh, Md. T. A. Ansari, and Md. S. Azam, “Fatigue life and damage evolution in woven GFRP angle ply laminates,” *International Journal of Fatigue*, Vol. 142, p. 105964, Jan. 2021, doi: 10.1016/j.ijfatigue.2020.105964.

[16] J. Brunbauer, C. Gaier, and G. Pinter, “Computational fatigue life prediction of continuously fibre reinforced multiaxial composites,” *Composites Part B: Engineering*, Vol. 80, pp. 269–277, Oct. 2015, doi: 10.1016/j.compositesb.2015.06.002.

[17] J. Hohe, M. Gall, S. Fliegener, and Z. M. A. Hamid, “A continuum damage mechanics model for fatigue and degradation of fiber reinforced materials,” *Journal of Composite Materials*, Vol. 54, no. 21, pp. 2837–2852, Sep. 2020, doi: 10.1177/0021998320904142.

[18] C. R. Kennedy, C. M. Ó. Brádaigh, and S. B. Leen, “A multiaxial fatigue damage model for fibre reinforced polymer composites,” *Composite Structures*, Vol. 106, pp. 201–210, Dec. 2013, doi: 10.1016/j.compstruct.2013.05.024.

[19] A. Matzenmiller, J. Lubliner, and R. L. Taylor, “A constitutive model for anisotropic damage in fiber-composites,” *Mechanics of Materials*, Vol. 20, no. 2, pp. 125–152, Apr. 1995, doi: 10.1016/0167-6636(94)00053-0.

[20] B. Mohammadi, B. Fazlali, and D. Salimi-Majd, “Development of a continuum damage model for fatigue life prediction of laminated composites,” *Composites Part A: Applied Science and Manufacturing*, Vol. 93, pp. 163–176, Feb. 2017, doi: 10.1016/j.compositesa.2016.11.021.

[21] T. Peng, Y. Liu, A. Saxena, and K. Goebel, “In-situ fatigue life prognosis for composite laminates based on stiffness degradation,” *Composite Structures*, Vol. 132, pp. 155–165, Nov. 2015, doi: 10.1016/j.compstruct.2015.05.006.

[22] Z. Feng, Q. Ma, H. Ma, Z. An, and Z. Bai, "A Common Model for Stiffness Degradation of Composites at Material and Product Levels," *J Fail. Anal. and Preven.*, Vol. 23, No. 4, pp. 1550–1557, Aug. 2023, doi: 10.1007/s11668-023-01692-x.

[23] K. Charlet, C. Baley, C. Morvan, J. P. Jernot, and J. Bréard, "Characteristics of Hermès flax fibres as a function of their location in the stem and properties of the derived unidirectional composites," *Composites Part A: Applied Science and Manufacturing*, Vol. 38, pp. 1912–1921, Aug. 2007, doi: 10.1016/j.compositesa.2007.03.006.

[24] A. Melelli, F. Jamme, D. Legland, J. Beaugrand, and A. Bourmaud, "Microfibril angle of elementary flax fibres investigated with polarised second harmonic generation microscopy," *Industrial Crops and Products*, Vol. 156, p. 112847, Nov. 2020, doi: 10.1016/j.indcrop.2020.112847.

[25] B. Xu, B. van den Hurk, S. J. D. Lugger, R. Blok, and P. Teuffel, "Creep analysis of the flax fiber-reinforced polymer composites based on the time–temperature superposition principle," *Science and Engineering of Composite Materials*, Vol. 30, No. 1, Jan. 2023, doi: 10.1515/secm-2022-0218.

[26] W. Claassen and G. Zarifis, "First Bio-Based Composite Movable Bicycle Bridge," *Structural Engineering International*, Vol. 31, No. 2, pp. 227–232, Apr. 2021, doi: 10.1080/10168664.2020.1840945.

[27] T. Jeannin, X. Gabrion, E. Ramasso, and V. Placet, "About the fatigue endurance of unidirectional flax-epoxy composite laminates," *Composites Part B: Engineering*, Vol. 165, pp. 690–701, May 2019, doi: 10.1016/j.compositesb.2019.02.009.